New Horizons in Earth Reinforcement – Otani, Miyata & Mukunoki (eds)
© 2008 Taylor & Francis Group, London, ISBN 978-0-415-45775-0

Physical and numerical modeling of EPS geofoam buffers for seismic load reduction on rigid walls

S. Zarnani
GeoEngineering Centre at Queen's-RMC, Department of Civil Engineering, Queen's University, Kingston, Ontario, Canada

R.J. Bathurst
GeoEngineering Centre at Queen's-RMC, Department of Civil Engineering, Royal Military College of Canada, Kingston, Ontario, Canada

ABSTRACT: The paper describes a series of experimental shaking table tests carried out at RMC to demonstrate that expanded polystyrene (EPS) geofoam materials can be used as seismic buffers to attenuate earthquake-induced dynamic forces developed against rigid retaining wall structures. Two different numerical modeling approaches are described that were used to predict the results of the physical experiments. The methods are based on: 1) a simple displacement block wedge approach, and; 2) a FLAC code. Both numerical approaches are shown to capture the peak dynamic-force time response of the seismic buffer wall models. The paper demonstrates both proof of concept and successful modeling approaches that can be used to predict load attenuation during earthquake using suitably selected EPS seismic buffers.

1 INTRODUCTION

Previous research has shown that the magnitude of static earth pressures against rigid wall structures can be reduced by placing a compressible vertical inclusion between the rigid wall and the retained soil.

One of the first reported field applications was described by Partos & Kazaniwsky (1987). In their study a prefabricated expanded polystyrene beaded drainage board 250 mm thick was placed between a 10-m high non-yielding basement wall and a granular backfill. Horizontally compressible platens were used by McGown et al. (1988) to construct 1-m high laboratory wall models in order to measure the effect of wall material compressibility on the magnitude of earth pressures and wall deformations. Physical test results reported by McGown & Andrawes (1987) and McGown et al. (1988) were used by Karpurapu & Bathurst (1992) to verify a non-linear finite element model (FEM) numerical approach. The numerical model was then used to develop a series of design charts for prototype-scale walls. The design charts can be used to select the thickness and elastic modulus of the compressible inclusion to minimize end-of-construction earth pressures against non-yielding retaining walls constructed to different heights and with a range of granular backfill materials compacted to different densities. A suitably selected vertical inclusion will allow sufficient lateral expansion of soil (controlled yielding) such that the retained soil is at or close to active failure and hence the earth pressures against the rigid structure are (according to classical earth pressure theory) at a minimum value.

Block-molded low-density expanded polystyrene (EPS) is the product of choice for the vertical compressible inclusion material today. EPS is classified as a geofoam material in modern geosynthetics terminology (Horvath 1995). A logical extension of the application of these systems to static load environments is the use of a geofoam inclusion for attenuation of seismic-induced dynamic earth loads. Specifically, potentially larger earth forces that develop during earthquakes can be reduced by a properly selected EPS geofoam material. In this paper, we refer to the compressible material as a seismic buffer.

Inglis et al. (1996) reported the first application of this technology in North America for seismic design. Panels of EPS from 450 to 610 mm thick were placed against rigid basement walls up to 9 m in height at a site in Vancouver, British Columbia. Their numerical analyses using program FLAC (Itasca 1996) showed that a 50% reduction in lateral loads could be expected during a seismic event compared to a rigid wall solution.

This paper first briefly describes an experimental test program that was carried out at the Royal Military College of Canada (RMC) to demonstrate proof of concept using the results of reduced-scale shaking table tests on rigid walls constructed with and without EPS geofoam seismic buffers.

Two different numerical model approaches were developed and verified against selected test results. The first is a simple displacement model and the second is a dynamic finite difference approach using the program FLAC. The paper shows that the results of both numerical models are in generally good agreement with experimental measurements.

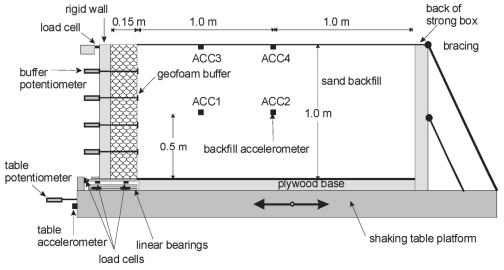

Figure 1. Example shaking table test configuration and instrumentation.

2 EXPERIMENTAL INVESTIGATION

2.1 *Reduced-scale shaking table tests*

A bulkhead (rigid wall) with height of 1 m and width of 1.4 m was constructed at the front of a strongbox mounted on a shaking table at RMC. Granular backfill soil was placed in the strongbox to a distance 2 m beyond the model wall. A total of seven different tests were carried out. Figure 1 illustrates an example experimental test set up showing the arrangement of the non-yielding wall, geofoam seismic buffer, retained soil and instrumentation. No geofoam seismic buffer was installed in Wall 1 (control). In all other walls the geofoam buffer had a constant thickness of 0.15 m.

One of the key material properties that define the compressive behavior of geofoam is its density. Many relationships are proposed in the literature that correlate the density of the geofoam to its initial elastic tangent Young's modulus. A summary of these correlations for non-elasticized geofoam has been reported by Zarnani & Bathurst (2007). Elasticized EPS is manufactured by applying a load-unload cycle after manufacture. This process makes the EPS geofoam linear elastic up to about 10% strain during compression (i.e. strains are recoverable) and linear (proportional) up to about 40% strain. Non-elasticized EPS is linear elastic up to about 1% strain. However, at the same density the elasticized EPS geofoam has a lower elastic modulus compared to the non-elasticized material. Properties of the EPS geofoam material used in the shaking table experimental tests are summarized in Table 1.

Due to page limitations only the experimental results for Walls 1, 2, 3 and 7 are presented in this paper. Walls 2 and 3 were constructed with commercially available EPS geofoam with nominal densities of 16 and 12 kg/m^3, respectively. For Wall 7, the density and hence the stiffness of the seismic buffer was artificially reduced by mechanically removing material from the EPS panels. Additional details and experimental results can be found in the papers by Bathurst et al. (2007a) and Zarnani & Bathurst (2007).

The backfill soil that was used for the experimental program was an artificial sintered synthetic olivine material (JetMag 30–60) which is silica-free and thus does not pose a health danger due to silica dust during material handling in an enclosed laboratory environment. Backfill soil properties are summarized in Table 2. The sand backfill was placed in 200-mm thick lifts and gently vibro-compacted using the shaking table. The same volume and placement technique was used in all of the experimental tests in order to have a consistent retained soil mass.

The rigid wall was made out of a 6-mm thick aluminum plate with aluminum stiffeners in all tests. Four load cells were used to rigidly brace the aluminium bulkhead to the shaking table platform. The entire wall system (bulkhead and seismic buffer) was seated on an instrumented footing supported by three frictionless linear bearings that were seated on five load cells. This arrangement made it possible to decouple the vertical and horizontal loads at the wall boundaries. The boundary conditions for the rigid wall prevented wall rotation and vertical and horizontal displacements. The lateral deformations at the geofoam-soil interface were measured by four potentiometers. The acceleration-time excitation history of the shaking table platform was measured by an accelerometer that was attached directly to the shaking table. In addition, four other accelerometers were embedded in the backfill soil at the locations shown in Figure 1.

The target base input excitation that was applied to all experimental tests was a stepped-amplitude sinusoidal record with a frequency of 5 Hz (Figure 2). This frequency (i.e. 0.2 s period) at 1/6-model scale corresponds to 2 Hz (i.e. 0.5 s period) at prototype scale according to the scaling laws proposed by Iai (1989). Frequencies of 2 to 3 Hz are representative of typical predominant frequencies of medium to high frequency earthquakes (Bathurst & Hatami 1998), and fall within the expected earthquake parameters for North American seismic design (AASHTO 2002). The displacement amplitude (i.e. actuator stroke) was increased at about 5-second intervals up to peak base acceleration amplitude in excess of 0.8 g and the test

Table 1. EPS geofoam buffer properties.

Wall #	Bulk density (kg/m^3)	Initial tangent Young's modulus (MPa)	Thickness (m)	Type (ASTM C 578)
1		Control structure (rigid wall with no seismic buffer)		
2	16	4.8$^{\#}$ (5.08 ± 1.89)‡	0.15	I
3	12	3.2$^{\#}$ (3.31 ± 1.48) ‡	0.15	XI
4	14	1.3$^{\#}$	0.15	Elasticized
5	6† (50% removed by cutting strips)	0.53$^{\#}$	0.15	XI
6	6† (50% removed by coring)	0.6$^{\#}$	0.15	XI
7	1.32† (89% removed by coring)	0.38$^{\#}$	0.15	XI

Notes: † density of intact EPS geofoam = 12 kg/m^3; $^{\#}$ average back-calculated values from cyclic stress-strain measurements during experiments; ‡ average modulus and standard deviation using published correlations with density (Bathurst et al. 2007a).

Table 2. Backfill soil properties.

Property	Value
Density	15.5 Mg/m^3
Peak angle of friction	51°
Residual friction angle	46°
Cohesion	0
Relative density	86%
Dilation angle	15°

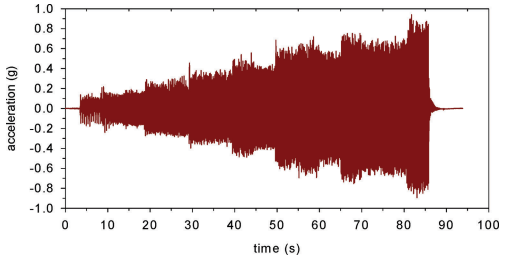

Figure 2. Example measured stepped-amplitude sinusoidal base excitation record – filtered to 12 Hz and linear baseline corrected.

terminated. This simple base excitation record is more aggressive than an equivalent true earthquake record with the same predominant frequency and amplitude. However, it allowed all walls to be excited in the same controlled manner and this allowed valid quantitative comparisons to be made between different wall configurations. Finally, it should be noted that the models were only excited in the horizontal cross-plane direction to be consistent with the critical orientation typically assumed for seismic design of earth retaining walls (AASHTO 2002).

2.2 *Experimental results*

The most important parameter to illustrate the relative influence of the seismic buffer on system response

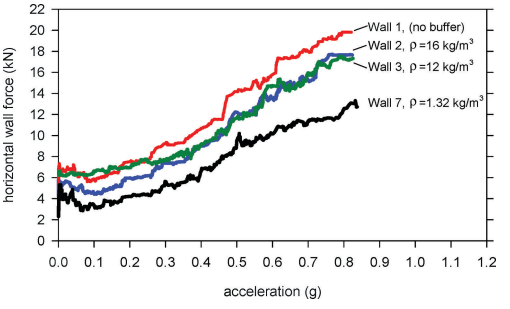

Figure 3. Horizontal wall forces recorded at peak base acceleration amplitude levels for Walls 1, 2, 3 and 7.

was the maximum lateral wall force-base acceleration history recorded at end of construction (initial static loading condition) and during subsequent excitation (Figure 3). The results illustrate that the control wall (Wall 1 with no seismic buffer) had the highest earth force and the model with the lowest bulk density geofoam buffer (Wall 7) had the lowest earth force. In order not to clutter the figure only the maximum horizontal wall force-peak base acceleration values at each stepped amplitude level are plotted in Figure 3. By installing an EPS seismic buffer at the back of the rigid wall in Walls 2, 3 and 7 the total lateral earth load was reduced by 11%, 15% and 40% of the value for the control wall, respectively, at peak acceleration of 0.75 g.

3 NUMERICAL MODELING

3.1 *Displacement model*

A simple one-block model was proposed by Bathurst et al. (2007b) to predict the dynamic response of the seismic buffer retaining walls described in the previous sections (Figure 4). This model is used here to simulate the experimental shaking table tests reported earlier.

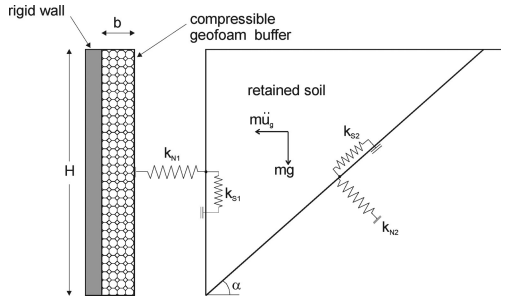

Figure 4. Single block displacement model.

In this model the soil wedge is considered as a rigid block under plane strain conditions. The displacement of the soil wedge is defined by horizontal and vertical displacements computed at the center of gravity of the mass. The small vertical deformations are ignored. The seismic buffer is located between the rigid retaining wall and soil. The failure plane in the backfill soil is assumed to be linear and to propagate from the heel of the buffer. A closed-form solution based on the classical Mononabe-Okabe wedge method was used to compute the wedge angle α (Bathurst et al. 2007b). This angle becomes smaller as the magnitude of horizontal acceleration increases. Linear spring models are used to compute the forces at the wedge boundaries as shown in Figure 4. A single linear compression-only spring is located at the geofoam-soil boundary.

During simulation runs this spring developed compression-only forces. The linear normal spring acting at the soil-soil wedge boundary permits tension and compression but was observed to develop only compressive forces during computation cycles. In order to allow plastic sliding at the block boundaries, the shear springs are modeled as stress-dependent linear-slip elements. An explicit time-marching finite difference approach that is commonly used for the solution of discrete element problems was used to solve the equations of motion for the sliding block. At each time step, the numerical scheme involves the solution of the equations of motion for the block followed by calculation of the forces.

Computed force-time responses for three test configurations with a compressible geofoam inclusion are presented in Figures 5a, 5b and 5c for Wall 2, 3 and 4, respectively. For clarity, only the peak values from the load-time records for each numerical simulation are plotted in the figures. The forces shown in these figures are the result of dynamic loading only. In other words, the datum for the plots is the end of construction.

The peak measured wall forces shown in Figure 5 are deduced from the sum of the readings from the horizontal load cells mounted against the back of the walls. There is generally good agreement between the physical and numerical models up to peak base input

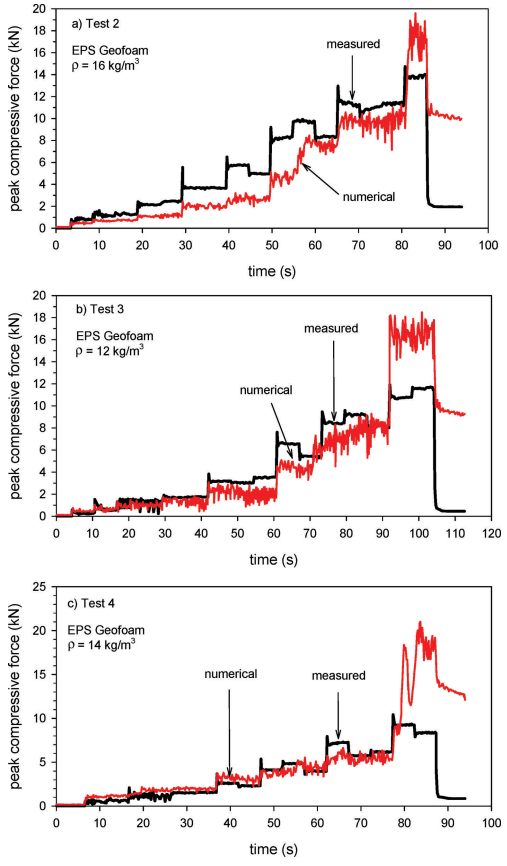

Figure 5. Wall force-time histories from physical tests and simple displacement numerical model.

acceleration of about 0.7 g. At higher accelerations there are likely more complex system responses that cannot be captured by the simple displacement model employed. For example, there are likely higher wall deformation modes at higher levels of base excitation. Nevertheless, the trends in the measured buffer force data for the three walls are generally captured by the numerical model up to about 0.7 g, and in many instances there is good quantitative agreement.

3.2 *FLAC modeling*

Program FLAC (Itasca 2005) was also used to simulate the RMC reduced-scale model walls. Figure 6 illustrates the FLAC numerical grid and boundary conditions used for the simulation of the geofoam buffer tests. The height and width of the numerical grid and thickness of the geofoam were kept the same as the physical tests.

The backfill soil was modeled as a purely frictional, elastic-plastic material with Mohr-Coulomb

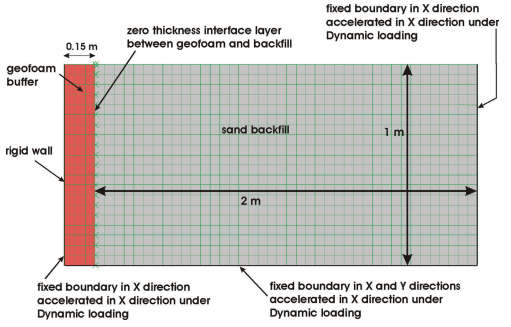

Figure 6. Numerical grid showing geofoam buffer, sand backfill and boundary conditions.

failure criterion. This model allows elastic behavior up to yield (Mohr-Coulomb yield point defined by the friction angle), and plastic flow at post-yield under constant stress. The geofoam buffer material was modeled as a linear elastic, purely cohesive material. While a more advanced non-linear strain hardening model could have been implemented in the FLAC code, the simple constitutive model adopted here was judged to be sufficient since the measured compressive strains in the physical models were less than the elastic strain limit of 1% determined from rapid uniaxial compression tests reported by the manufacturer. A constant Rayleigh damping ratio of 3% was used for the whole system at a frequency equal to the predominant frequency of the model (20 Hz).

The rough bottom boundary in the physical tests (i.e. a layer of sand was epoxied to the bottom of the strong box container) was simulated with a no-slip boundary at the bottom of the sand backfill. The interface between the buffer and the soil was a slip and separation boundary with zero thickness. The measured base excitation record during experiments for each test was applied to the base and the two vertical boundaries of the numerical models. The horizontal input acceleration was applied in the form of an equivalent velocity record (i.e. integrated acceleration record) with baseline correction to ensure zero displacement at the base at the end of shaking.

The peak magnitudes of horizontal wall force predicted at the end of construction and during base excitation of numerical models were investigated. The variation of maximum wall force with time for three physical tests and numerical simulations are presented in Figure 7. The vertical axis in the plots corresponds to the total horizontal earth force acting against the rigid wall per unit width of wall. The figures show that there is reasonably good agreement between measured and predicted results. There is a noticeable discrepancy between results at the beginning of the test for Wall 3. This is believed to be due to locked-in initial horizontal stresses that may have developed as a result of the

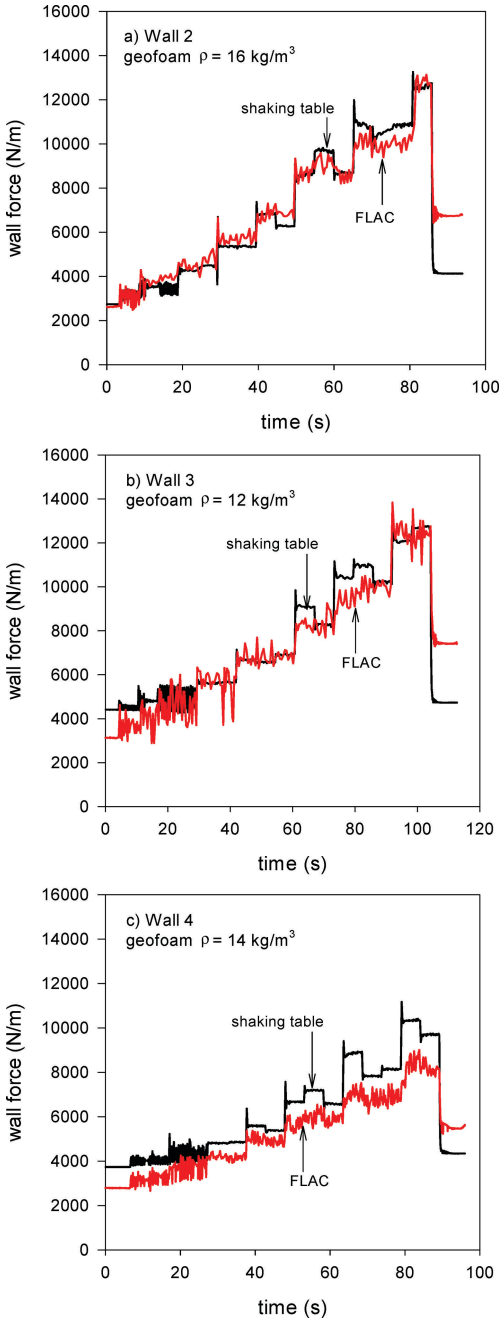

Figure 7. Wall force-time histories from physical tests and FLAC numerical simulations.

initial vibro-compaction technique that was used to densify the soil during placement of the sand layers in the strong box. The numerical model results are consistently lower than the physical test results for Wall

4 but the overall qualitative trends are in good agreement. The discrepancy is believed to be related to the selection of dynamic elastic modulus value used in the numerical model which was back-calculated from measured displacements and wall forces (Zarnani & Bathurst 2007).

4 CONCLUSIONS

A series of shaking table experimental tests are described that were carried out on 1-m high model rigid walls with and without a geofoam seismic buffer. The physical experiments demonstrate that a properly selected vertical compressible inclusion of EPS geofoam placed against a rigid retaining wall can be used to attenuate dynamic earth forces due to simulated earthquake. In this experimental program, modified EPS materials reduced dynamic loads by up to 40%.

Two different numerical approaches are described that can be used to simulate geofoam seismic buffer performance. One model is based on a sliding block approach and the other uses a dynamic finite difference approach implemented within a FLAC code. Both approaches captured the trend in measured data and in most cases there was good agreement between numerical and experimental results.

ACKNOWLEDGMENTS

The work described in this paper was supported by a research grant from the Natural Sciences and Engineering Research Council of Canada held by the second author.

REFERENCES

AASHTO, 2002. Standard Specifications for Highway Bridges. *American Association of State Highway and Transportation Officials*, Seventeenth Edition. Washington, DC, USA.

ASTM C 578-06, 2006. Standard Specification for Rigid Cellular Polystyrene Thermal Insulation. American Society for Testing and Materials, West Conshohocken, Pennsylvania, USA.

Bathurst, R.J. & Hatami, K. 1998. Seismic response analysis of a geosynthetic reinforced soil retaining wall. *Geosynthetics International* 5 (1&2): 127–166.

Bathurst, R.J., Hatami, K. & Alfaro, M.C. 2002. Geosynthetic-reinforced soil walls and slopes—seismic aspects. In: Shukla SK, editor, Geosynthetics and their applications, Thomas Telford, [chapter 14].

Bathurst, R.J., Zarnani, S. & Gaskin, A. 2007a. Shaking table testing of geofoam seismic buffers. *Soil Dynamics and Earthquake Engineering* 27 (4): 324–332.

Bathurst, R.J., Keshavarz, A., Zarnani, S. & Take, A. 2007b. A simple displacement model for response analysis of EPS geofoam seismic buffers. *Soil Dynamics and Earthquake Engineering* 27 (4): 344–353.

Horvath, J.S. 1995. *Geofoam Geosynthetic*, Horvath Engineering, P.C., Scarsdale, NY, 217 p.

Iai, S. 1989. Similitude for shaking table tests on soil-structure-fluid model in 1g gravitational field. *Soils and Foundations* 29: 105–118.

Inglis, D., Macleod, G., Naesgaard, E. & Zergoun, M. 1996. Basement wall with seismic earth pressures and novel expanded polystyrene foam buffer layer. *Tenth Annual Symposium of the Vancouver Geotechnical Society*, Vancouver, BC, Canada. 18 p.

Itasca Consulting Group, 1996, 2005. FLAC: Fast Lagrangian Analysis of Continua, version 3.3 and 5.0. Itasca Consulting Group, Inc., Minneapolis, Minnesota, USA.

Karpurapu, R. & Bathurst, R.J. 1992. Numerical investigation of controlled yielding of soil-retaining wall structures. *Geotextiles and Geomembranes* 11: 115–131.

McGown, A. & Andrawes, K.Z. 1987. Influence of wall yielding on lateral stresses in unreinforced and reinforced fills. *Research Report 113*, Transportation and Road Research Laboratory, Crowthrone, Berkshire, UK.

McGown, A., Andrawes, K.Z. & Murray, R.T. 1988. Controlled yielding of the lateral boundaries of soil retaining structures. In Proceedings of the *ASCE Symposium on Geosynthetics for Soil Improvement*, ed. R. D. Holtz, Nashville, TN, USA. pp. 193–211.

Partos, A.M. & Kazaniwsky, P.M. 1987. Geoboard reduces lateral earth pressures. In Proceedings of *Geosynthetics'87*, Industrial Fabrics Association International. New Orleans, USA. pp. 628-639.

Zarnani, S. & Bathurst, R.J. 2007. Experimental investigation of EPS geofoam seismic buffers using shaking table tests. *Geosynthetics International* 14 (3): 165–177.